MONITORING EARLY-AGE CRACK FORMATION IN A Ca-Fe-Al-RICH INORGANIC POLYMER

Glenn BEERSAERTS[1,2], Lukas ARNOUT[1], Lieven MACHIELS[1], Jan ELSEN[2], Yiannis PONTIKES[1]

[1] Department of Materials Engineering, KU Leuven, 3001 Heverlee, Belgium
[2] Department of Earth and Environmental Science, KU Leuven, 3001 Heverlee, Belgium

glenn.beersaerts@kuleuven.be, lukas.arnout@kuleuven.be, lieven.machiels@kuleuven.be, jan.elsen@kuleuven.be, yiannis.pontikes@kuleuven.be

Introduction

It is estimated that 8% of the anthropogenic CO_2 emission, a contributor to global warming, can be allocated to the production process of Ordinary Portland Cement (OPC).[1] Therefore, alternative binder systems are being investigated. One potential binder is inorganic polymers (IP), which can be produced by the alkali activation of a glassy precursor.[2] One possible precursor is a Ca-Fe-Al silicate glass, generated after quenching of a residual melt, which is formed *via* a gasification/vitrification process in a plasma surface, fuelled by municipal waste.[3] During the synthesis of the IP, several authors reported the formation of cracks, which can be caused by shrinkage of the IP.[4,5] Understanding crack formation and eventually mitigating the phenomenon, is one of the challenges in the field of IP.[4]

This paper investigates the driving forces for crack formation at early age in two IP mortars, synthesised with two different alkali solutions. Shrinkage and elasticity experiments were carried out to compare the properties of these two mortars. Furthermore, acoustic emission (AE) tests were performed to register the amount and intensity of cracks formed in each IP. Finally, these shrinkage, elasticity and AE results were correlated.

Materials and Methods

The Ca-Fe-Al silicate glass precursor has an amorphous phase content of >97% and a chemical composition of (in wt%): 33 SiO_2, 22 CaO, 20 Fe_2O_3, 12 Al_2O_3, 4 Na_2O, 3 MgO, 2 ZnO, 2 TiO_2 and 2 others, according to the XRF results.[5] Two alkali solutions were made, one consisting of 60 wt% H_2O and the other of 80 wt% H_2O, both with a molar SiO_2/K_2O ratio of 1.6, as shown in Table 1.

Table 1: Ratios of activating solutions and mortar

Activating solution			Mortar			
H_2O (wt%)	H_2O/K_2O (molar)	Density (g/cm^3)	Code	Liquid/Solid (kg/kg)	Liquid/ Solid (m^3/ m^3)	Glass/ Sand
60	15.85	1.53	60M	0.44	0.91	0.41
80	42.26	1.26	80M	0.37	0.91	0.41

The glass and the activating solution were mixed for two minutes. Afterwards, CEN standard sand (EN 196-1) was added and mixed for one minute. Next, the obtained mortars, 60M and 80M, were casted in a 10x20x5 cm^3 mould for elasticity and AE measurements. The mortars used for shrinkage measurement were casted in a 30 cm long and 8 cm diameter tube, up to a reference level. Before casting, a Teflon sheet was placed between the mortar and the tube to reduce friction. The temperature and humidity was not controlled, but both moulds were placed in an insulating chamber of around 23°C to prevent any major temperature and humidity fluctuations. The elasticity or E-modulus was measured by the emission of longitudinal pulses at a frequency of 500 kHz. The time delay of a pulse gave an indication for the elasticity or stiffness. The shrinkage behaviour of the IP mortars was measured by a Linear Variable Differential Transformer (LVDT). A Teflon floater was placed on the surface to measure a voltage difference by the LVDT, which was translated in a vertical displacement of the IP. Cracks were recorded by their AE. A crack produces an acoustic wave which travelled, through the sample, on metal bars, up to a sensor. Cracks were registered as hits, each with its own peak amplitude in decibel (dB), on a sensor frequency of 350 kHz.

Results and Discussion

The elasticity and macroscopic shrinkage results were combined and shown, for each sample, in Figure 1a and b. Two clear displacement trends can be identified for 60M and 80M. The first displacement trend can be allocated to autogenous shrinkage, which was a result of volume-reducing polymerisation reactions and drying shrinkage.[6] This shrinkage took place in the liquid-gel state because no stiffness was registered yet. The second trend was less evident and can be identified as expansion due to relaxation, when most exothermal polymerisation reactions were concluded, in the hardened state of the IP.[7] The increase in elasticity can be explained as the transformation from a liquid-gel phase into a hard phase.[8] The shrinkage values of 60M were significantly higher than 80M, implying that higher availability of K-silicates resulted in a larger amount of polymerisation reactions. The elasticity values for 80M were also lower. The retardation in elasticity development can be explained by a decrease in rate of network formation, as a result of the high H_2O/K_2O ratio in the activating solution. The AE results of 60M and 80M are presented in Figure 1c and d. More cracks were registered for 60M, compared to 80M, as shown in Figure 1c. An exponential increase in crack formation can be observed for 60M and 80M during the first 12 hours of measurement. Later in time, the exponential increase in the

cumulative number of cracks reached a plateau and hardly any more cracks were generated. Figure 1d shows that 60M produced cracks with a broader range of peak amplitudes, including higher peak amplitudes (65 dB up to 97 dB), in comparison with 80M. The majority of cracks produced in 80M have low peak amplitudes (40.5 dB). Cracks with a high peak amplitude can be identified as high energy cracks, which were interpreted as macro-cracks. Cracks with a low peak amplitude corresponded to low energy cracks, which were expected to be micro-cracks.[9]

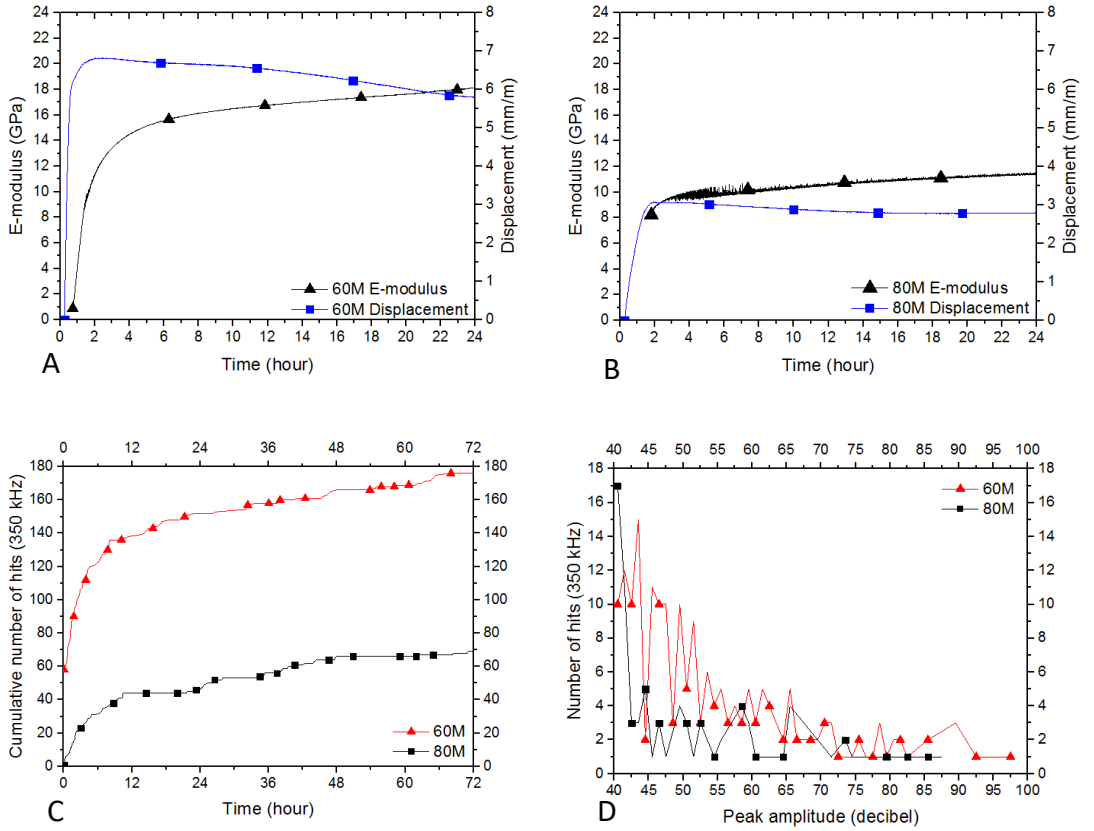

Figure 1: A and B present the shrinkage and elasticity or E-modulus results of 60M and 80M, C indicates the cumulative amount of hits or cracks registered in 60M and 80M, D shows the amount of hits for each peak amplitude (dB) in 60M and 80M

Considering all the data, the first shrinkage event phased out once a certain stiffness was attained. From that moment, the solid IP network could withstand shrinkage, while evaporation and self-desiccation took place in the pores. Consequently, capillary pressure in pores and differential stress in matrix heterogeneities were able to build up, which were exerted on the surface of the network.[10] Once the stress exceeded the strength, cracks were produced in the IP.[11] A faster stiffness increase in 60M resulted in higher stresses and the production of more macro-cracks during the first 12 hours of curing, in comparison with sample 80M. Afterwards, once a considerable strength was gained in the IP, stress build up in the sample did not result in cracks anymore and the cumulative crack number reached a plateau.

Conclusions

Ca-Fe-Al silicate glass was activated with two activating solutions, with varying water content, to investigate their influence on the shrinkage, elasticity and crack formation. A more K-silicate rich solution resulted in higher early age autogenous shrinkage and a faster elasticity development. Furthermore, the choice of the activating solution influenced the amount of cracks. At a certain elasticity, further shrinkage was inhibited, which induced stress in the IP through capillary pressure build up and matrix heterogeneities. A fast stiffness increase, induced a large amount of stress, which exceeded the early strength and produced macro-cracks. The production of cracks ceased, after 12 h of curing, once sufficient strength was generated in the IP.

References

1. J. Olivoer, G. Janssens-Maenhout, J. Peters, Trends in global CO_2 emissions; 2012 Report, PBL Netherlands Environmental Assessment Agency, The Hague, 2012.
2. A. Mellado, C. Catalán N. Bouzón, M. V. Borrachero, J. M. Monzó and J. Payá. "Carbon footprint of geopolymeric mortar: Study of the Contribution of the Alkaline Activating Solution and Assessment of an Alternative Route", *RSC Advances*, **4** 23846-23852 (2014).
3. L. Machiels, L. Arnout, P. Yan, P. T. Jones, B. Blanpain and Y. Pontikes, "Transforming Enhanced Landfill Mining Derived Gasification/Vitrification Glass into Low-Carbon Inorganic Polymer Binders and Building Products", *J Sustain Metall*, in press.
4. A. A. Melo Neto, M. A. Cincotto and W. Repette, "Drying and Autogenous Shrinkage of Pastes and Mortars with Activated Slag Cement", *Cem Concr Res*, **38** (4) 565–574 (2008).
5. L. Kriskova, L. Machiels and Y. Pontikes, "Inorganic Polymers from a Plasma Convertor Slag: Effect of Activating Solution on Microstructure and Properties", *J Sustain Metall*, **1** (3) 240–251 (2015).
6. N. P. Lee and BRANZ (Firm), *Creep and Shrinkage of Inorganic Polymer Concrete*, BRANZ (Firm), Porirua, 2007.
7. E. Holt, *Early Age Autogenous Shrinkage of Concrete*, Technical Research Centre of Finland, Espoo, 2001.
8. K. van den Abeele, W. Desadeleer, G. de Schutter and M. Wevers, "Active and Passive Monitoring of the Early Hydration Process in Concrete Using Linear and Nonlinear Acoustics", *Cem Concr Res*, **39** (5) 426-432 (2009).
9. A. Farhidzadeh, S. Salamone, B. Luna and A. Whittaker, "Acoustic Emission Monitoring of a Reinforced Concrete Shear Wall by b-value-based Outlier Analysis", *Struct Health Monit*, **12** (1) 3–13 (2013).
10. P. Turcry, A. Loukili, L. Barcelo and J. M. Casabonne, "Can the Maturity Concept be Used to Separate the Autogenous Shrinkage and Thermal Deformation of a Cement Paste at Early Age?", *Cem Concr Res*, **32** (9) 1443–1450 (2001).
11. D. P. Bentz and O. M. Jensen, "Mitigation Strategies for Autogenous Shrinkage Cracking", *Cem Concr Compos*, **26** (6) 677–685 (2004).